PHYSICAL REVIEW LETTERS

Strain-Dependent Deformation Behavior in Nanocrystalline Metals

Hongqi Li,[1,2,*] Hahn Choo,[2] Yang Ren,[3] Tarik A. Saleh,[1] Ulrich Lienert,[3] Peter K. Liaw,[2] and Fereshteh Ebrahimi[4]

[1]*Materials Science and Technology Division, Los Alamos National Laboratory, Los Alamos, New Mexico 87545, USA*
[2]*Department of Materials Science and Engineering, University of Tennessee, Knoxville, Tennessee 37996, USA*
[3]*Advanced Photon Source, Argonne National Laboratory, Argonne, Illinois 60439, USA*
[4]*Department of Materials Science and Engineering, University of Florida, Gainesville, Florida 32611, USA*
(Received 3 March 2008; published 3 July 2008)

The deformation behavior as a function of applied strain was studied in a nanostructured Ni-Fe alloy using the *in situ* synchrotron diffraction technique. It was found that the plastic deformation process consists of two stages, undergoing a transition with applied strain. At low strains, the deformation is mainly accommodated at grain boundaries, while at large strains, the dislocation motion becomes probable and eventually dominates. In addition, current results revealed that, at small grain sizes, the 0.2% offset criterion cannot be used to define the macroscopic yield strength any more. The present study also explained the controversial observations in the literature.

Nanocrystalline materials possess a variety of unique physical and mechanical properties due to their fine grain sizes and, therefore, have been the theme of many studies [1–4]. As far as the deformation mechanism is concerned, it has been accepted that the deformation mechanism exhibits a transition from dislocation activity to grain boundary sliding at a critical grain size. The critical value is defined as the breakdown point in the Hall-Petch plot, and this breakpoint has been calculated to occur at 15–20 nm for face-centered cubic (fcc) metals [5,6]. To date, the typical approaches to uncover the nanometals' deformation mechanism include calculation of activation volume [7], TEM characterization [8–10], and computer simulation [5,6,11–13]. Generally, the activation volume measures the average volume of dislocation structures involved in the deformation process. In the case of TEM straining, the areas examined are usually near a crack tip, where the local strain is high [14]. Regarding the computer simulation, the deformation behavior is characterized as a function of grain size by studying a series of materials with different grain sizes. In addition, near the critical grain size, the deformation transition proceeds gradually, and the plastic deformation is a combination of dislocation and grain boundary activities. It is obvious that the deformation behavior at different strains is still poorly understood and open to discussion, and the reported approaches did not separate the contribution of each mechanism to plasticity. The aim of this Letter is to study the dependence of deformation behavior on applied strains in a nanocrystalline Ni-Fe alloy.

In this study, *in situ* neutron and synchrotron scatterings were employed to study the deformation behavior of single-phase fcc coarse-grained Ni and a nanograined Ni−15 wt % Fe alloy, respectively. Neutron and high-energy synchrotron scatterings have strong penetration capabilities and are capable of investigating the deformation mechanism at the grain size level in bulk specimens.

Today, they have been employed to study the deformation behavior of nanostructured and large-grained composites [15,16] and conventional metals [17,18] as well as the lattice strain distribution within individual dislocation cells [19].

The Ni−15 wt % Fe alloy was made via electrodeposition [20]. TEM characterizations showed that the grain size ranged from 4 to 30 nm, and no columnar grains developed during the electrodeposition [21]. Based on the measurement of about 1000 grains, the average grain size is about 9 nm, which is below the critical grain size value of about 14 nm for Ni-Fe alloys [22]. Figure 1 presents the stress-strain curves acquired during the *in situ* neutron or synchrotron tensile tests. The macroscopic 0.2% offset yield stresses are 215 and 1475 MPa for Ni and the Ni−15 wt % Fe alloy, respectively. The nanocrystalline Ni−15 wt % Fe
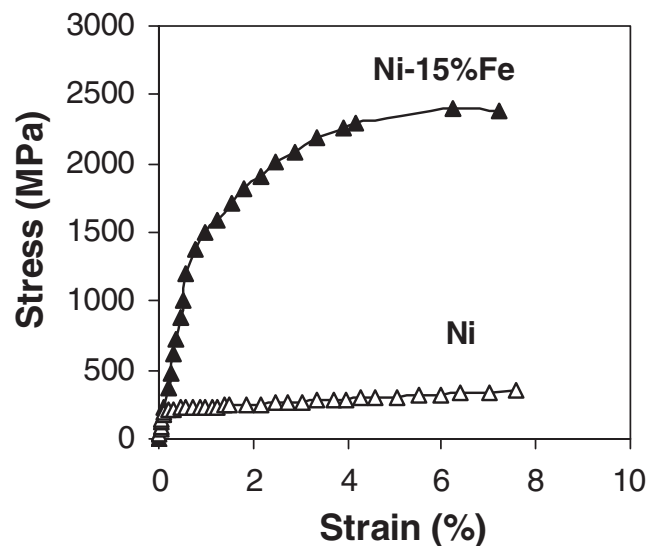

FIG. 1. Tensile stress-strain curves of the coarse-grained Ni and nanograined Ni−15 wt % Fe alloy.

alloy's plastic strain is as large as 6.1%, which includes a 5% uniform tensile elongation. Current data are consistent with our previous reports for the same alloy [4,21]. The large plasticity enables us to study the evolution of deformation mechanism from small to large strains. For the coarse-grained Ni, the specimens were loaded beyond the 5% plastic strain.

Figure 2 shows the lattice strains parallel to the loading direction as a function of applied stress for Ni and the Ni– 15 wt % Fe alloy, where the dotted lines denote the 0.2% yield strength. The lattice strain ε^{hkl} is calculated from the change in lattice spacing d^{hkl}: $\varepsilon^{hkl} = (d^{hkl} - d_0^{hkl})/d_0^{hkl}$, where d^{hkl} and d_0^{hkl} are the d spacings at a given applied stress and a low-load reference point, respectively. It can be seen that within the elastic regime, in both cases, the lattice strain increases linearly with increasing the applied stress,

following Hooke's law. Above the yield stresses, substantial deviations from the elastic linearity occurred due to plastic anisotropy. In a single-phase material, when plastic deformation starts, dislocation slips operate first within the grain sets with the slip system oriented preferentially to the loading axis, while other grain sets continue to deform elastically. As a result, the applied load is partitioned to the grain sets that have not plastically deformed yet. Such load redistribution results in the lattice strain departure from the linear evolution [17,18]. In general, the grain family that has plastically deformed shows a compressive shift, while those grain sets that have not plastically deformed yet exhibit a tensile shift. For the fcc metals, plastic deformation begins in grains next to the [220] orientation [17], resulting in that the {220} grain family demonstrated a compressive shift (upward inflection), as seen in Fig. 2(a). On the other hand, the [200] orientation is the most compliant and stays elastic the longest. As a result, the {200} grain family carries more loads after plastic deformation and, thus, exhibited a tensile shift (downward inflection), as shown in Fig. 2(a). These observations are consistent with the reported results for other coarse-grained fcc metals [17,18]. However, in the case of the nanocrystalline Ni– 15 wt % Fe alloy, all of the lattice planes exhibited tensile shifts (downward inflection) after the plastic deformation occurred, as shown in Fig. 2(b). Current observations indicate that the deformation mechanism changes with the grain size.

For fcc metals, the [200] and [220] orientations have the most significant deflections from the linearity so that they are usually emphasized to study the deformation behavior [16–18]. In Fig. 3, the lattice strain deviations of the [200] and [220] orientations from the elastic linearity are plotted as a function of the normalized applied stress (the applied
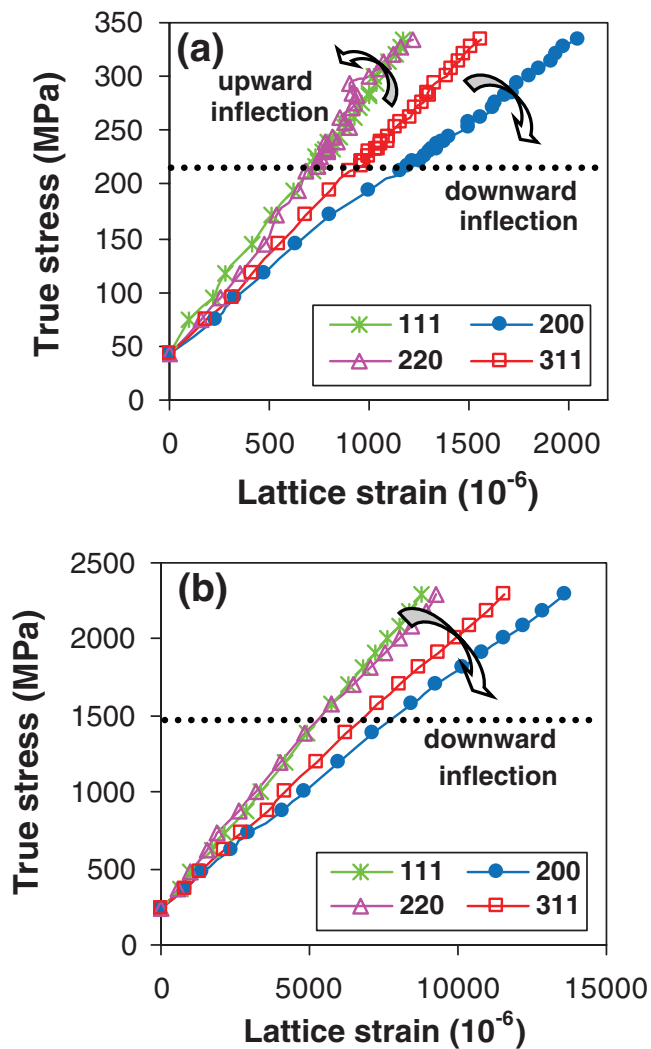

FIG. 2 (color). The lattice strain evolutions along the loading direction as a function of the applied stress. (a) Coarse-grained Ni. (b) Nanograined Ni–15 wt % Fe alloy. The dotted lines mark the 0.2% yield stresses.
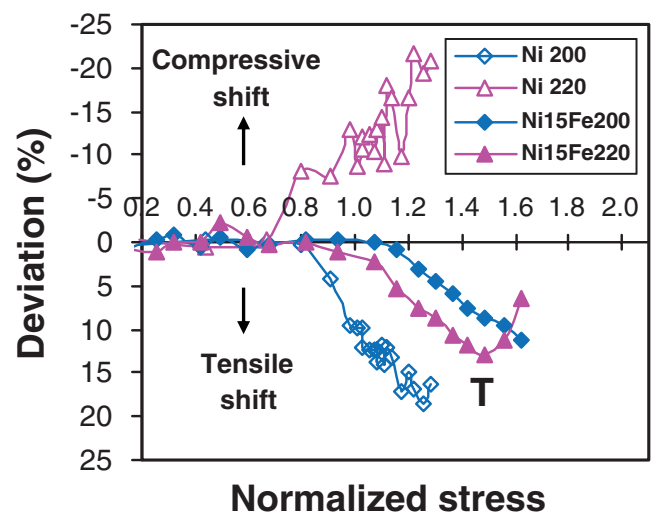

FIG. 3 (color). The deviation of the lattice strains from the elastic linearity as a function of the normalized stress (applied stress divided by yield stress).

stress divided by the yield stress). Apparently, like other coarse-grained materials, Ni demonstrates a pronounced deviation prior to the 0.2% yield stress. A close analysis discloses that the remarkable deviations started at a normalized stress between 0.7 and 0.8. This Ni's elastic limit is about 170 MPa, corresponding to a normalized stress of 0.79. Typically, the start point of noticeable deviations in the lattice strain-true stress curves manifests the onset of plastic deformation [15–18]. Therefore, these results indicate that, for coarse-grained Ni, the onset of macroscopic plasticity is consistent with the beginning of microscopic plastic deformation. However, for the nanocrystalline Ni–15 wt % Fe alloy, the obvious lattice strain shift from the linearity started at a stress beyond the 0.2% yield stress. The calculation found that the lattice strain's linearity ended at a plastic strain of 0.5%. That is, the macroscopic 0.2% offset yield criterion does not reflect the beginning of microscopic deformation and probably cannot be used to determine the onset of plasticity in nanostructures [23].

Furthermore, Fig. 3 shows that, for the nanograined Ni–15 wt % Fe alloy, both [200] and [220] orientations demonstrated tensile shifts, which is different from the phenomenon observed in the conventional fcc metals and cannot be understood by the dislocation slip mechanism. It is known that, at small grain sizes, the fraction of grain boundary atoms is significant. Consequently, nanostructures are usually considered as composites consisting of crystalline grain cores and either an amorphous grain boundary "phase" [24] or a crystalline coating [25]. Unlike the load redistribution behavior (between different crystallographic orientations) in a single-phase material, for composites, the load redistribution takes place between different phases. Generally, the hard phase bears greater loads [15,16]. Thus, the hard phase exhibits a tensile shift, and the soft phase shows a compressive shift. In the case of nanostructures' composite models, at the grain sizes below critical values, the grain boundary is softer than the grain core [24,25] so that the grain boundary phase deforms first when the deformation enters the plastic regime. As a result, all of the lattice strains measured from the crystalline cores exhibit tensile shifts, as seen in Figs. 2 and 3. The grain boundary phase would exhibit a compressive shift. It is worth mentioning that the grain boundary phase is not an actual phase in the sense that the grain boundary atoms are just less ordered than those in grain cores. Therefore, this phase does not show distinct diffraction peaks in the diffraction patterns. The current results are also supported by simulation results that, for 5.2 nm Cu, after plastic deformation, the tensile stress developed inside grains, and compressive stress built up at grain boundaries [13].

It is interesting that in Fig. 3, at the point **T** (corresponding to a plastic strain of 2.2%), the [220] orientation starts to deflect toward the compressive shift direction, while the [200] orientation continues in the tensile shift direction. This deviation behavior is the same as what has been observed in the large-grained fcc metals. That is, the load partitioning takes place between different crystallographic orientations. This finding suggests that, at large strains, the dislocations begin to make a dominant contribution to the plasticity. It is known that, at large strains, further plastic deformation needs large applied stresses due to the strain hardening. On the other hand, for nanostructured metals, the stress accumulated in grain interiors is larger than that at grain boundaries, and the larger stress builds up in larger grains [13]. Furthermore, at large strains, the stress concentration can develop at triple junctions [25]. A combination of these three factors can ineluctably facilitate and enhance the dislocation activities in larger grains. The current results indicate that, at grain sizes near the critical value, the dislocation activities would intensify if a larger plasticity can be realized. This rationale has been verified by recent studies [26–28]. For instance, numerous dislocations can be found in the cold-rolled nanostructured fcc metals, where a severe plastic deformation larger than 30% was introduced by rolling [26]. In addition, recent simulation results suggest that, at the grain size about 10 nm, the contribution of dislocations to plastic deformation increases with increasing the plastic strain [27,28], while the grain boundary sliding's contribution decreases at large strains [28]. Moreover, the present results also rationalized a puzzled observation in the literature. For example, *in situ* TEM straining results show that, surprisingly, extensive dislocation activities are still prevalent in 10 nm grains [10]. The current study suggests that such intensive dislocation activities may be attributed to the local stress concentration near the crack tip.

Besides dislocation and grain boundary activities, deformation twinning may also occur during plastic deformation. However, the twinning is less favorable due to high unstable twin fault energy [29,30], especially at ambient temperature and quasistatic strain rates [29]. More importantly, the deformation twins in the fcc nanometals originate from the motion of partial dislocations and may not contribute to macroscopic strains [31]. Furthermore, the introduction of twins mainly affects the x-ray diffraction peak's intensity (i.e., texture) and full width at half maximum (i.e., internal strain) and does not affect the peak position (i.e., lattice strain) [27]. As a result, the current discussion based on the deviation features of lattice strains is not affected by the existence of deformation twins.

In summary, the *in situ* neutron and synchrotron diffraction investigations on the coarse- and nanograined Ni alloys were conducted. The results show that, at a small grain size below the critical value, the deformation mechanism depends on the applied strain. At small strains, the plasticity is predominately accommodated at grain boundaries. However, at large strains (>2.2%), the dislocations start to play an important role in the plastic deformation. Furthermore, current characterization also disclosed that, in nanocrystals, the 0.2% offset criterion is no

longer appropriate for determining the macroscopic yield strength. Finally, current findings propose a novel deformation scenario, which provided new insights to the deformation mechanisms at small grain sizes.

*To whom correspondence should be addressed. hqli@lanl.gov.

[1] J. R. Weertman, D. Farkas, K. Hemker, H. Kung, M. Mayo, R. Mitra, and H. Van Swygenhoven, MRS Bull. **24**, 44 (1999).

[2] K. M. Youssef, R. O. Scattergood, K. L. Murty, and C. C. Koch, Appl. Phys. Lett. **85**, 929 (2004).

[3] K. S. Kumar, H. Van Swygenhoven, and S. Suresh, Acta Mater. **51**, 5743 (2003).

[4] H. Li and F. Ebrahimi, Appl. Phys. Lett. **84**, 4307 (2004).

[5] J. Schiøtz and K. W. Jacobsen, Science **301**, 1357 (2003).

[6] V. Yamakov, D. Wolf, S. R. Phillpot, A. K. Mukherjee, and H. Gleiter, Philos. Mag. Lett. **83**, 385 (2003).

[7] H. Q. Li, H. Choo, and P. K. Liaw, J. Appl. Phys. **101**, 063536 (2007).

[8] M. Ke, S. A. Hackney, W. W. Milligan, and E. C. Aifantis, Nanostruct. Mater. **5**, 689 (1995).

[9] Z. Shan, E. A. Stach, J. M. K. Wiezorek, J. A. Knapp, D. M. Follstaedt, and S. X. Mao, Science **305**, 654 (2004).

[10] R. C. Hugo, H. H. Kung, R. Mitra, J. R. Weertman, J. Knapp, and D. Folstaedt, Acta Mater. **51**, 1937 (2003).

[11] V. Yamakov, D. Wolf, S. R. Phillpot, A. K. Mukherjee, and H. Gleiter, Nat. Mater. **3**, 43 (2004).

[12] H. Van Swygenhoven, P. M. Derlet, and A. Hasnaoui, Phys. Rev. B **66**, 024101 (2002).

[13] J. Schiøtz, F. D. Di Tolla, and K. W. Jacobsen, Nature (London) **391**, 561 (1998).

[14] Q. Z. Chen, H. Q. Li, and W. Y. Chu, Mater. Lett. **38**, 367 (1999).

[15] L. Thilly, P. O. Renault, V. Vidal, F. Lecouturier, S. Van Petegem, U. Stuhr, and H. Van Swygenhoven, Appl. Phys. Lett. **88**, 191906 (2006).

[16] T. S. Han and P. R. Dawson, Mater. Sci. Eng. A **405**, 18 (2005).

[17] B. Clausen, T. Lorentzen, and T. Leffers, Acta Mater. **46**, 3087 (1998).

[18] M. R. Daymond, C. N. Tomé, and M. A. M. Bourke, Acta Mater. **48**, 553 (2000).

[19] L. E. Levine, B. C. Larson, W. Yang, M. E. Kassner, J. Z. Tischler, M. A. Delos-Reyes, R. J. Fields, and W. Liu, Nat. Mater. **5**, 619 (2006).

[20] H. Q. Li and F. Ebrahimi, Acta Mater. **51**, 3905 (2003).

[21] H. Q. Li and F. Ebrahimi, Acta Mater. **54**, 2877 (2006).

[22] C. Cheung, F. Djuanda, U. Erb, and G. Palumbo, Nanostruct. Mater. **5**, 513 (1995).

[23] S. Brandstetter, H. Van Swygenhoven, S. Van Petegem, B. Schmitt, R. Maass, and P. M. Derlet, Adv. Mater. **18**, 1545 (2006).

[24] H. S. Kim, Scr. Mater. **39**, 1057 (1998).

[25] S. Benkassem, L. Capolungo, and M. Cherkaoui, Acta Mater. **55**, 3563 (2007).

[26] X. L. Wu and E. Ma, Appl. Phys. Lett. **88**, 231911 (2006).

[27] S. Brandstetter, P. M. Derlet, S. Van Petegem, and H. Van Swygenhoven, Acta Mater. **56**, 165 (2008).

[28] N. Q. Vo, R. S. Averback, P. Bellon, S. Odunuga, and A. Caro, Phys. Rev. B **77**, 134108 (2008).

[29] X. L. Wu, Y. T. Zhu, and E. Ma, Appl. Phys. Lett. **88**, 121905 (2006).

[30] H. Van Swygenhoven, P. M. Derlet, and A. G. Frøseth, Nat. Mater. **3**, 399 (2004).

[31] X. L. Wu, X. Z. Liao, S. G. Srinivasan, F. Zhou, E. J. Lavernia, R. Z. Valiev, and Y. T. Zhu, Phys. Rev. Lett. **100**, 095701 (2008).